PMMA-Modified Divinylester/Styrene Resins: Phase Diagrams and Morphologies

Walter F. Schroeder,[1] María J. Yáñez,[2] Mirta I. Aranguren,[1] Julio Borrajo[1]

[1]*Department of Chemical Engineering, Institute of Research in Materials Science and Technology (INTEMA), Universidad Nacional de Mar del Plata, Mar del Plata 7600, Argentina*
[2]*Regional Center of Basic and Applied Research (CRIBABB), Camino La Carrindanga Km. 7 8000, Bahía Blanca, Argentina*

Received 29 March 2005; accepted 24 June 2005
DOI 10.1002/app.22511
Published online in Wiley InterScience (www.interscience.wiley.com).

ABSTRACT: Binary and ternary experimental cloud-point curves (CPCs) for systems formulated with a low molar mass synthesized divinylester (DVE) resin, styrene (St), and poly(methyl methacrylate) (PMMA) were determined. The CPCs results were analyzed with the Flory–Huggins (F-H) thermodynamic model taking into account the polydispersity of the DVE and PMMA components, to calculate the different binary interaction parameters and their temperature dependences. The St-DVE system is miscible in all the composition range and down to the crystallization temperature of the St; therefore, the interaction parameter expression reported for a higher molar mass DVE was adapted. The interaction parameters obtained were used to calculate the phase diagrams of the St-PMMA and the DVE-PMMA binary systems and that of the St-DVE-PMMA ternary system at three different temperatures. Quasiternary phase diagrams show liquid–liquid partial miscibility of the St-PMMA and DVE-PMMA pairs. At room temperature, the St-DVE-PMMA system is miscible at all compositions. Final morphologies of PMMA-modified cured St-DVE materials were generated by polymerization-induced phase separation (PIPS) mechanism from initial homogeneous mixtures. SEM and TEM micrographs were obtained to analyze the generated final morphologies, which showed a direct correlation with the initial miscibility of the system. © 2006 Wiley Periodicals, Inc. J Appl Polym Sci 100: 4539–4549, 2006

Key words: divinylester resin; PMMA modifier; blends; phase diagrams; Flory–Huggins analysis; morphology

INTRODUCTION

Thermosetting polymers formulated with divinylester (DVE) resins are extensively used in a vast range of applications that require rigid materials resistant to high temperatures and solvents. Such applications range from biomedical (for dental implants and bone cements) to industrial supplies (for the construction of ship hulls, car bodyworks, and equipment for the chemical industry).[1] During the manufacturing process, these resins are copolymerized with an unsaturated monomer, usually styrene (St).[1]

As in the case of other thermosetting matrices,[2,3] those obtained with DVE are fragile and, during forming, undergo a high volumetric shrinkage.[4,5] These drawbacks can be partially overcome with the addition of modifying additives of the elastomeric or thermoplastic type. Usually, the modifying method consists of preparing a reactive homogeneous mixture of St and DVE comonomers and the modifying additive. During the St-DVE copolymerization reaction, in the presence of the modifier, a phase separation occurs because of the reduction of entropic contribution to the mixing Gibbs free energy due to the copolymer formation, the change in the relative concentrations of comonomers and the formed copolymer, and the increase in the degree of crosslinking. The morphology developed, determined by the size, shape, and relative proportions of the domains of the phases present in the heterogeneous system, influences the thermal, mechanical, and fracture properties of the material obtained.[5–10]

The understanding of the thermodynamic phase behavior of the system is important because the miscibility of these systems and their evolution during the cure reaction determine, to a great extent, the material's final morphology. The control of developed morphology is of the utmost importance to regulate the material toughness without causing an important deterioration of the final thermal and mechanical properties of the material.

During copolymerization, the reaction system is constituted by four components: unreacted St and DVE comonomers, formed (St-*co*-DVE) copolymer,

Correspondence to: J. Borrajo (jborrajo@fi.mdp.edu.ar).
Contract grant sponsor: CONICET.
Contract grant sponsor: ANPCyT.
Contract grant sponsor: National University of Mar del Plata.

and modifier. The phase transformation diagram is represented by a tetrahedron with one component in each vertex. The St-DVE-modifier triangular face of the tetrahedron represents the phase behavior for the reaction system at zero conversion and constitutes the ternary phase diagram for the physical mixture of the three initial components.

Different studies on similar reaction systems formulated with St, unsaturated polyester (UP) prepolymers, and low-profile additives (LPA) such as poly(methyl methacrylate) (PMMA) or poly(vinyl acetate) (PVAc)[7,11–13] demonstrate that the morphology developed can be correlated with the position of the initial reaction mixture on the corresponding ternary phase diagram. Therefore, the knowledge of these phase diagrams can help to understand the effect of the temperature, composition, and reaction kinetics variables on the generated morphologies.

In the few thermodynamic studies reported on the miscibility of binary and ternary systems formulated with St and DVE, elastomeric poly(butadiene-*co*-acrylonitrile) additives terminated in vinyl (VTBN), carboxyl (CTBN), or epoxy (ETBN) groups[14,15] were used. To our knowledge, there are no published thermodynamic studies with thermoplastic modifiers such as PMMA or PVAc that have been used with excellent results to achieve the "low-profile" effect in UP.[16–18]

In this work, the miscibilities of the quasibinary systems as well as the St-DVE-PMMA quasiternary systems at different temperatures were determined by measuring their cloud-point curves (CPCs), which were further analyzed with the Flory–Huggins (F-H) lattice theory. Finally, the ultimate morphologies of the materials obtained were investigated and analyzed in relation to the initial miscibility of the reaction mixtures.

THEORETICAL BACKGROUND

In this work, the simplest version of F-H lattice theory was applied considering the binary interaction parameters as inversely proportional to temperature and composition independent, and taking into account the effect of each component polydispersity.

A convenient starting point for the thermodynamic description of polymer blends is the F-H expression for the dimensionless mixing Gibbs free energy per mole of lattice sites[19–21]

$$\frac{\Delta G^{\mathrm{mix}}}{MRT} = \sum_{i}\sum_{j=1}^{N_i}\frac{\phi_{ij}}{r_{ij}}\ln\phi_{ij} + \sum_{i<k}\chi_{ik}\phi_i\phi_k \qquad (1)$$

where the symbols $i, k = 1,2,3$ represent components; $j = 1,2,\ldots,Ni$ the total number of different molecular species corresponding to the i component; ϕ_{ij} is the volume fraction of the j molecular species of the i component, ϕ_i is the total volume fraction of the i component; and $\chi_{ik} = \chi_{ki}$ is the binary interaction parameter, which is only temperature-dependent. The M factor represents the total mole number of lattice sites and is given by $M = \sum_{i}\sum_{j=1}^{N_i} n_{ij}r_{ij}$, where n_{ij} is the number of moles of the j-mer of the i component; and r_{ij} is its relative molar volume, defined as $r_{ij} = V_{ij}/V_r$ V_{ij} represents the molar volume of the j molecular species of the i component, and V_r the reference volume, which, in this study, was taken as the molar volume of the St monomer.

For a generic ij molecular species, the dimensionless chemical potential difference between the polymer solution state and the pure state, per mole of lattice sites, is defined thermodynamically in the usual form,

$$\frac{\Delta\mu_{ij}}{r_{ij}RT} = \left[\frac{\partial(\Delta G^{\mathrm{mix}}/MRT)}{\partial n_{ij}}\right]_{P,T,n_{km\neq ij}} = \frac{1}{r_{ij}} + \frac{\ln\phi_{ij}}{r_{ij}} - \sum_{i}\sum_{j=1}^{N_i}\frac{\phi_{ij}}{r_{ij}} + \sum_{k\neq i}\chi_{ik}\phi_k(1-\phi_i) - \chi_{kl}\phi_k\phi_l \qquad (2)$$

where $i(k,l) = 1,2,3$ are the components in a quasiternary system, and $i(k) = 1,2$ with $\phi_l = 0$ in a quasibinary. In this work, the binary interaction parameter, χ_{ik}, was assumed to be inversely proportional to the temperature and composition independent, given by the usual linear equation

$$\chi_{ik} = a_{ik} + \frac{b_{ik}}{T} \qquad (3)$$

where a_{ik} and b_{ik} are characteristic constants that represent the residual entropic and enthalpic contributions, respectively, for a particular ik binary system.[19–21]

Under constant temperature and pressure, thermodynamic requirements for the liquid–liquid phase equilibrium in a mixture with polydisperse components are expressed by the identity of chemical potentials of each molecular species between the two liquid phases

$$\Delta\mu_{ij}^{\alpha} = \Delta\mu_{ij}^{\beta} \qquad (4)$$

where α and β represent the mother and emergent phases in equilibrium at the cloud-point conditions, respectively. In addition, an equation for the mass balance for the β-emergent phase must be included in this analysis. This balance is given by

$$\sum_{i}\phi_i^{\beta} = 1 \qquad (5)$$

TABLE I
Physicochemical Characteristics of the Used Components

	M_n (g/mol)	M_w/M_n	r_n	r_w	r_z	Density at 25°C (g/cm^3)
St (1)	104	1.00	1.0	1.0	1.0	0.914[a]
DVE (2)	600[b]	1.06	4.8	5.1	5.5	1.157[a]
PMMA (3)	41,500[b]	1.93	317.0	612.2	898.8	1.188[c]

[a] Measured using a precision balance for densities.
[b] Measured by SEC.
[c] Taken from the supplier's catalog.

with $\phi_i^{\beta} = \sum_{j=1}^{N_i} \phi_i^{\alpha} W_{ij} \exp(r_{ij}\sigma_i)$ for a polydisperse polymer component and $\phi_i^{\beta} = \phi_i^{\alpha} \exp(r_i \sigma_i)$ for a monodisperse or single component. W_{ij} is the mass fraction molecular species distribution of the i polymer in the α-mother phase, since at the cloud-point condition, only an infinitesimal amount of polymer is segregated to the emergent phase, and σ_i is the separation factor of the i component, whose value determines the extension of the fractionation of each molecular species between the two equilibrium phases and is defined by the liquid–liquid equilibrium equations of both α and β phases.

The general phase equilibrium and mass balance conditions must be solved simultaneously to obtain the CPC and the shadow curve (ShC).

The spinodal curve (SC) represents the stability limit of the homogeneous quasibinary or quasiternary mixtures, and the critical solution point (CSP) is the intercept of the CPC, the ShC, and the SC, where the two separate phases become identical in composition and form one phase mixture. The resulting equations used in the calculation of SC and CSP in polydisperse polymer solutions have been previously reported in the literature.[14,19–21]

EXPERIMENTAL

Materials and preparation of blends

A DVE monomer was synthesized from the reaction of an epoxy resin diglycidyl ether of bisphenol A (DGEBA, DER 332, Dow Chemical Co.; epoxy equivalent weight 175 g/equiv.) with methacrylic acid (Norent Plast S.A., Buenos Aires, Argentina, laboratory-grade reagent) and triphenylphosphine (Fluka A.G., Switzerland; analytical reagent) as catalyst. The final conversion reached (monitored by titration of residual acid groups and by FTIR (Mattson Genesis II)) was higher than 97%, and the final product was stabilized with 500 ppm of hydroquinone.

The obtained monomer was characterized by FTIR and ^{1}H-NMR (Bruker AM-500) spectroscopies,[4,22] and its molar mass was measured by SEC chromatography (Waters Model 440, with columns PLGel of 100, 500, 10^3, 10^4, and 10^6Å) in distilled tetrahydrofuran (Laboratorios Cicarelli, Argentina; analytical reagent) with a flow rate of 1 mL/min, using polystyrene calibration. The SEC chromatogram also allowed to obtain the molecular species distribution of the synthesized DVE. Finally, its density was determined using a precision balance (Becker and Sons).

Table I summarizes the physicochemical characterization of all the components used in this work.

The PMMA modifier utilized was supplied by Aldrich Chemical Company. Its molar mass and molecular species distribution were measured by SEC (Waters ALC 244, with columns Shodex A 802, 803, 804, 805, and 806/S) with refraction index and specific viscosity detection on line (Viscotek Model 200), using universal calibration.

The final morphologies were observed in samples of the obtained materials from crosslinking reaction of the DVE with St (Poliresinas San Luis S.A., Argentina; laboratory-grade reagent) using benzoyl peroxide 2 wt % (Lucidol 75%, Akzo Chemicals S.A., Buenos Aires, Argentina) as initiator, and with added PMMA as modifier. The PMMA particles were initially dissolved in part of the St and then they were mixed with the DVE and the remaining St to reach the final composition.

Plaques of 3-mm thickness were cast between glass plates coated with a silicone release agent, spaced by a rubber cord and held together with clamps. The temperatures and times employed in the full cure schedule were: (a) 50°C for 2 h to degas the sample; (b) a cure temperature of 80°C for 1 h 30 min; and finally, (c) a postcure at 150°C for 2 h. After this process, the samples were cooled slowly in the oven.

Cloud point and phase diagrams

The cloud-point temperatures of the binary physical mixtures were determined from solutions with different known compositions, by observing the point of change from transparency to cloudiness or vice versa, by varying the mixture temperature under moderate agitation. Each measurement was repeated at least five times to account for reproducibility. The temperature was registered with an alcohol thermometer with 1°C precision. The measured cloud points are represented

as the nonisothermal experimental points in the binary phase diagram.

For ternary systems, cloud-point compositions were obtained by a titration method. Initially, St-DVE-PMMA mixtures of known global concentrations were prepared. A fixed volume of each mixture was introduced in a glass cylinder with jacket and thermostatized at a fixed temperature by a fluid circulating in the jacket supplied from an external thermostatic bath. The mixture was titrated with an St-DVE binary solution of known concentration from a burette with 0.1 cm^3 precision. Because the measurements were carried out at temperatures below room temperature, the system was isolated with a polyethylene wrapping and the water vapor was expulsed by dry nitrogen current to prevent its condensation inside the system. The measurement of the amount of solution required, from the burette, to achieve the point of change "cloudy to transparent" or vice versa allows the calculation of the cloud-point concentration in each test; and all measured points generate the CPC in the ternary phase diagram at constant temperature.

Electron microscopy

Liquid nitrogen fractured specimens were coated with a gold layer (30 nm) in a sputter coater (PELCO 91000) and observed in a scanning electron microscope (JEOL JSM-35 CF, Japan) with a secondary electron detector. A 15-kV accelerating voltage and 6000× magnification were used.

Samples to be studied by transmission electron microscopy (TEM) were sectioned in a LKB ultramicrotome with a diamond knife. The rigidity of the obtained materials was high enough to prepare high-quality ultrathin sections at room temperature. The section thickness was 60 nm for all samples studied to compare the different morphologies. This study was performed on a JEOL 100 CX transmission electron microscope (Japan) operating at 80 kV. All micrographs were taken with the same magnification (10,000×).

RESULTS AND DISCUSSION

CPCs were fitted with the simplest version of F-H lattice model, which considers the binary interaction parameter as inversely proportional to the temperature and independent of the concentration and molar mass of the polymers (eq. (3)).

The thermodynamic analysis was carried out using the method developed by Kamide and coworkers, for quasibinary and quasiternary systems.[19,20,23] To increase the convergence velocity of the method and to reduce the calculation time, the experimental continuous distributions of molar masses of the polydisperse polymers were replaced by discrete distributions of pseudocomponents.[24] This scheme led to essentially the same average molar masses M_n, M_w, M_z, as the original distributions. Besides, the predictions for selected thermodynamic systems resulted in very good agreement with that obtained from continuous distributions. According to this, discrete distributions were adapted in the rest of the analysis.

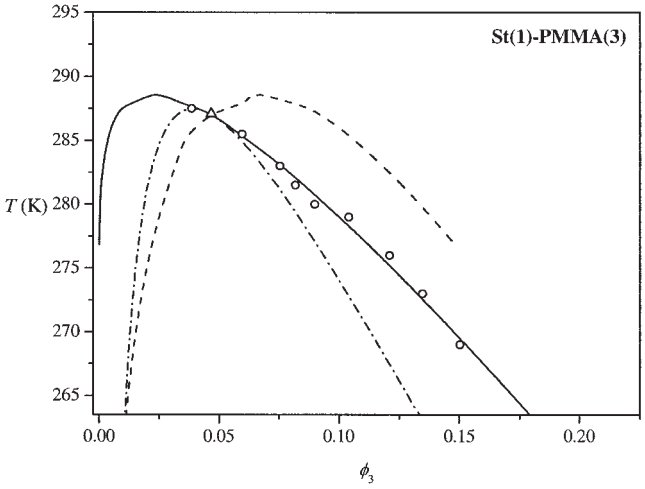

Figure 1 Phase diagram of the St(1)-PMMA(3) quasibinary system: (○○) experimental cloud points; (—) calculated CPC; (– –) calculated ShC; (– · –) calculated SC; (·) calculated CSP.

Quasibinary systems

St(1)-PMMA(3)

Figure 1 shows the experimental cloud-point phase diagram for the St(1)-PMMA(3) quasibinary system. As it can be seen, this system presents an upper critical solution temperature (UCST) behavior. The immiscibility region inside the measured CPC envelope is very similar to that obtained by us, in a previous work[21] for the same system, but using a PMMA of higher molar mass and polydispersity index (M_n = 239,000 g/mol; M_w/M_n = 2.68). This result indicates that the miscibility of this system is less affected by the molar mass of PMMA in the studied range.

The experimental cloud-point phase diagram was analyzed with eqs. (2), (4), and (5) to obtain the value of interaction parameter at each measured temperature. During the resolution, the Schulz–Zimm distribution function, which was used to represent the distribution of PMMA molecular species, was approximated by one discrete distribution with 30 pseudocomponents adequately defined. The CSP and the critical interaction parameter (which are strongly dependent on the distribution function[19]) calculated with the discretization method (ϕ_{3c} = 0.0469; T_c = 287.02 K) are in very good agreement with those obtained using the continuous distribution (ϕ_{3c} =

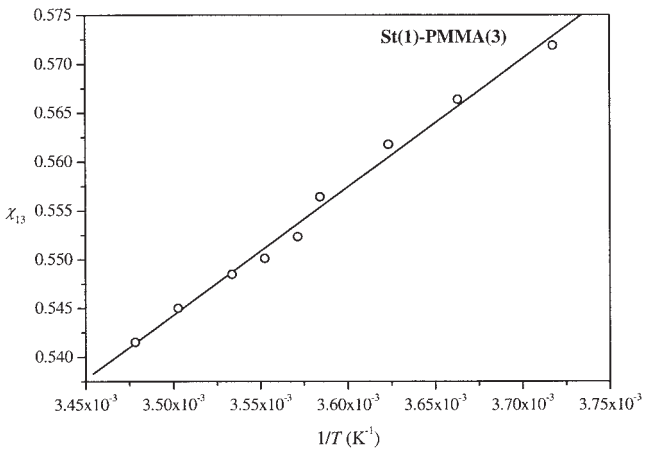

Figure 2 Temperature dependence of the St(1)-PMMA(3) binary interaction parameter: (○) values calculated from the measured cloud points; (—) results of the linear regression equation.

0.0467; T_c = 287.15 K). Figure 2 shows the calculated χ_{13} values versus $1/T$. As it can be observed, a very good linear correlation was obtained in agreement with eq. (3). The constants a and b obtained from a linear fitting are listed in Table II.

Calculated CPC, ShC, SC, and CSP for the St(1)-PMMA(3) quasibinary system are shown in Figure 1. They were obtained from the inverse calculation using $\chi_{13}(T)$ values given by eq. (3). By comparing experimental and calculated CPCs, it can be concluded that, despite its simplicity, the F-H theory with this χ-parameter equation describes very well the experimental quasibinary cloud-point phase diagram for this system.

St(1)-DVE(2)

The experimental cloud points corresponding to the liquid–liquid phase separation in St(1)-DVE(2) solutions could not be measured during cooling, because the low molar mass of the synthesized DVE monomer greatly increases the miscibility in this system. Covering a wide range of compositions studied, all the prepared solutions remained homogeneous even at temperatures down to 242 K, at which the St crystallization was observed.

In the framework of the F-H lattice model, the binary interaction parameter is considered only temperature dependent, and not concentration or molar mass dependent. Under this assumption, it is possible to assign to this system the same χ-parameter expression obtained by Auad et al.,[14] using solutions of St and a commercial DVE of higher molar mass and polydispersity index (M_n = 1015 g/mol, M_w/M_n = 1.74). In that work, the effect of DVE monomer polydispersity was considered by defining 40 pseudocomponents for the molar mass distribution measured by SEC.

The constants a and b assumed to define the interaction parameter expression for this system are listed in Table II. The ability of this $\chi(T)$ expression to represent correctly the St-(lower molar mass) DVE interaction parameter was further confirmed by using it in the analysis of the quasiternary cloud-point phase diagrams.

DVE(2)-PMMA(3)

The experimental cloud points corresponding to the liquid–liquid phase separation in DVE(2)-PMMA(3) solutions could not be measured with a satisfactory reproducibility. The high viscosity of this system at low temperatures, (the temperature range at which it was expected that the phase separation took place[21]), made extremely difficult the expulsion of the microbubbles generated during stirring, and this turned the cloud-point determination very difficult. For this reason, the expression for the interaction χ-parameter for this quasibinary system was obtained from the thermodynamic analysis of the experimentally measured CPCs for the St-DVE-PMMA quasiternary system at different temperatures.

Figures 3–5 show the experimental cloud-point phase diagrams for the St(1)-DVE(2)-PMMA(3) quasiternary system at three different temperatures: 253, 260, and 265 K, respectively. An increase in the miscibility regions can be seen when temperature increases, in accordance with an UCST behavior. At room temperature, the system is completely miscible at all compositions.

Combination of the required thermodynamic condition for the liquid–liquid phase equilibrium, eq. (4), the expression for the chemical potential of an ij generic molecular species, eq. (2), and the mass balance equation for the β-emergent phase, eq. (5), allows to write a system of three equations with five unknown variables (χ_{23}, ϕ_1^{α}, ϕ_2^{α}, ϕ_1^{β}, and ϕ_2^{β}). At a fixed temperature, χ_{23} is a constant value that can be obtained from each experimental (ϕ_1^{α}, ϕ_2^{α}) ternary cloud-point value. For each temperature, a single value of the χ_{23}-parameter was determined averaging the calculated values obtained from each measured ternary cloud point. This calculation method was repeated at each temperature.

TABLE II
Constants a and b of the Binary Interaction Parameter Equation

Binary pair	a	b (K)
St(1)-PMMA(3)	0.085	131.3
St(1)-DVE(2)[a]	−0.330	325.1
DVE(2)-PMMA(3)	−2.498	705.1

[a] Taken from the reference [14].

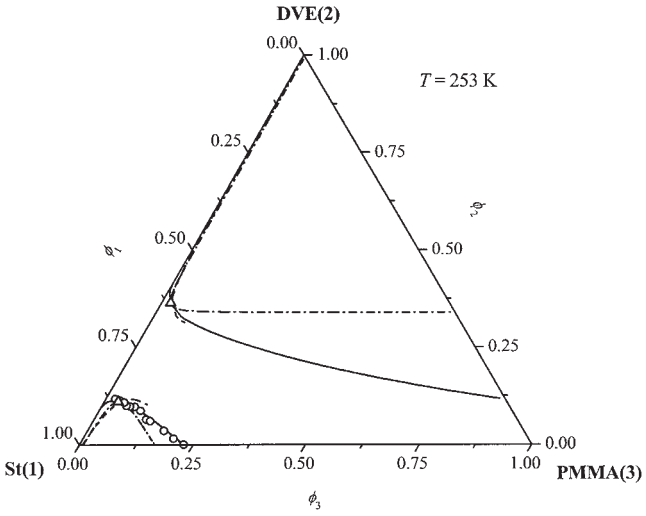

Figure 3 Phase diagram of the St(1)-DVE(2)-PMMA(3) quasiternary system at 253 K: (○○) experimental cloud points; (—) calculated CPC; (– –) calculated ShC; (– · –) calculated SC; (·) calculated CSP.

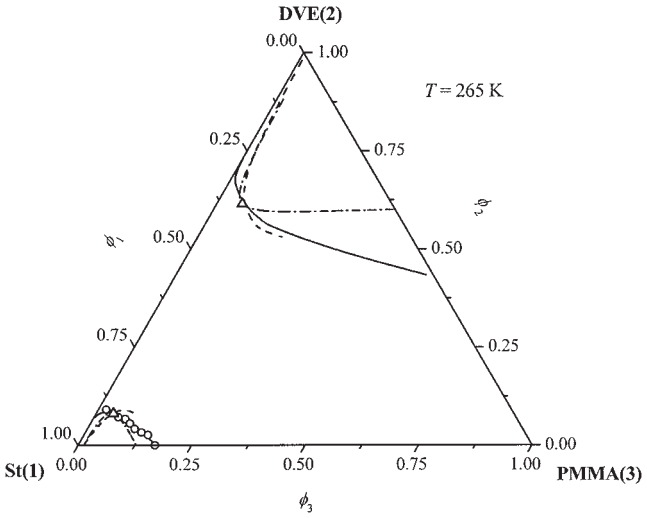

Figure 5 Phase diagram of the St(1)-DVE(2)-PMMA(3) quasiternary system at 265 K: (○○) experimental cloud points; (—) calculated cloud point curve; (– –) calculated ShC; (– · –) calculated SC; (·) calculated CSP.

During the calculations, the mass-fraction distribution obtained from the SEC chromatogram of the synthesized DVE was approximated by one discrete distribution including 40 pseudospecies. The average relative molar sizes calculated with the discrete distribution (r_n = 4.82; r_w = 5.08; and r_z = 5.52) are in very good agreement with those obtained from original complete SEC distribution (r_n = 4.83; r_w = 5.10; and r_z = 5.54). The PMMA polydispersity was represented by the same distribution function used in the St-PMMA quasibinary analysis.

Figure 6 shows the calculated χ_{23}-parameter values versus $1/T$, obtained from the measured ternary systems at the three different temperatures. The interaction parameter constants, a and b, for this quasibinary system were obtained from a linear fitting of the calculated values and are reported in Table II. These values were used to perform the calculation of the DVE(2)-PMMA(3) quasibinary cloud-point phase diagram, which could not be experimentally measured. Figure 7 shows the calculated phase diagram in which the immiscibility region is located at low temperatures as was expected. By comparing this calculated phase diagram with that measured for a similar system but using a higher molar mass DVE (M_n = 1015 g/mol, M_w/M_n = 1.74),[21] it is observed that the increase in

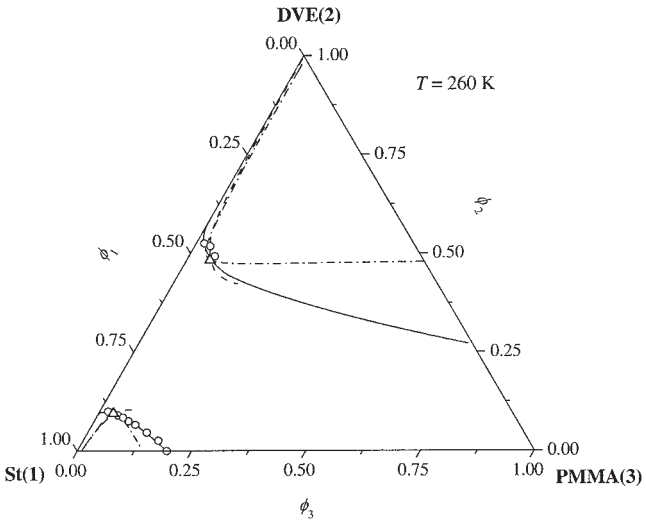

Figure 4 Phase diagram of the St(1)-DVE(2)-PMMA(3) quasiternary system at 260 K: (○○) experimental cloud points; (—) calculated CPC; (– –) calculated ShC; (– · –) calculated SC; (·) calculated CSP.

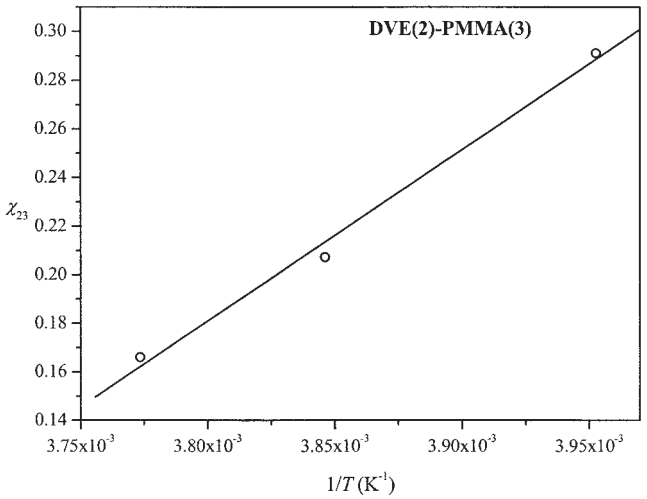

Figure 6 Temperature dependence of the DVE(2)-PMMA(3) binary interaction parameter: (○) calculated values from the measured ternary cloud points; (—) results of the linear regression equation.

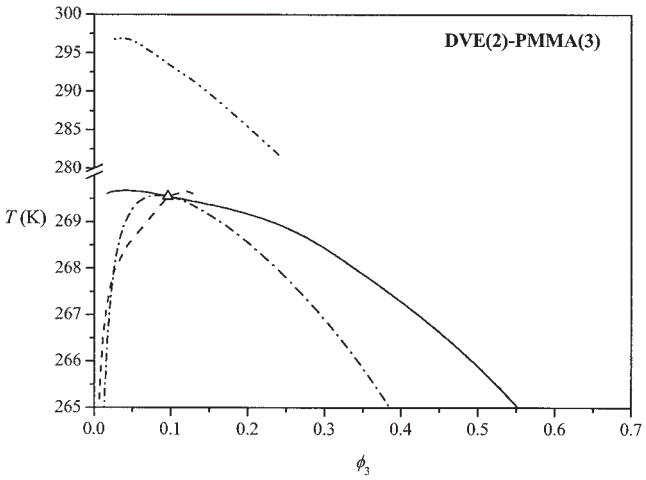

Figure 7 Calculated phase diagram of the DVE (M_n = 600 g/mol)(2)-PMMA (M_n = 41,500 g/mol)(3) quasibinary system: (—) CPC; (– –) ShC; (– · –) SC; (·) CSP. (– · · –) CPC for a DVE (M_n = 1015 g/mol)-PMMA (M_n = 41,500 g/mol) quasibinary system included for comparison.

DVE molar mass causes a displacement of the cloud-point phase diagram to higher temperatures, thereby increasing the immiscibility area. This effect is originated by the reduction of the entropic contribution to the mixing Gibbs free energy, caused by the increase in the DVE molecular size. In Figure 7, the CPC for the higher molar mass DVE is included for comparison.

Analysis of the St(1)-DVE(2)-PMMA(3) quasiternary system

During the thermodynamic analysis, it was assumed that the residual part of the mixing Gibbs free energy for the quasiternary system, eq. (1), is constituted by the addition of the quasibinary residual contributions taken into account through the previously obtained binary interaction χ-parameters. The combination of the condition for the phase equilibrium, eq. (4), the expression for the chemical potentials, eq. (2), and the mass balance for the β-phase, eq. (5), leads to a system of three equations with four unknown variables that can be solved numerically for the unknown independent global compositions, $(\phi_1^{\alpha},\phi_2^{\alpha})$ and $(\phi_1^{\beta},\phi_2^{\beta})$, assuming one of them as fixed. In this way, it is possible to calculate the compositions for the two liquid phases in equilibrium at the cloud-point condition. The locus of these compositions determine the CPC for the α-mother phase and the ShC for the β-emergent phase. For the calculations, each polydisperse component was represented by the same discrete distribution that was used in the analysis of the quasibinary systems.

Figures 3–5 show the calculated CPCs, ShCs, SCs, and CSPs for the St(1)-DVE(2)-PMMA(3) quasiternary system at 253, 260, and 265 K, respectively. As it can be observed, a very good agreement between the experimental and calculated CPCs is obtained. It is interesting to note that the immiscibility region originated in the DVE-PMMA binary axis varies more noticeably with temperature than that originated in the St-PMMA binary axis. This difference is caused principally by the higher values of the b constant, which represents a higher endotherm enthalpic contribution to the interaction parameter in the DVE-PMMA quasibinary, in comparison with that for the St-PMMA.

Final morphologies of the modified networks

Final materials were obtained by the crosslinking reaction between the St and DVE comonomers at 80°C, with PMMA added as a modifier. In this work, the typical commercial concentrations of comonomers and additives were used, taken a fixed weight proportion of St : DVE = 45 : 55, modified with 5–20 wt % PMMA. Points in Figure 8 represent formulations with 5, 10, 15, and 20 wt % PMMA on the quasiternary phase diagram. In this diagram, the immiscibility regions enclosed by the cloud-point phase equilibrium curves at 253, 260, and 265 K are showed. As it can be seen, the ternary immiscibility area decreases when temperature increases, as it corresponds to an UCST behavior. At room temperature and at the cured temperature (80°C), the ternary system is initially miscible at all compositions. This behavior was experimentally confirmed, since the unreacted mixtures exist macroscopically as one homogeneous phase at room temperature.

During copolymerization, the phase state of the St-DVE-PMMA-(St-*co*-DVE) copolymer reaction system

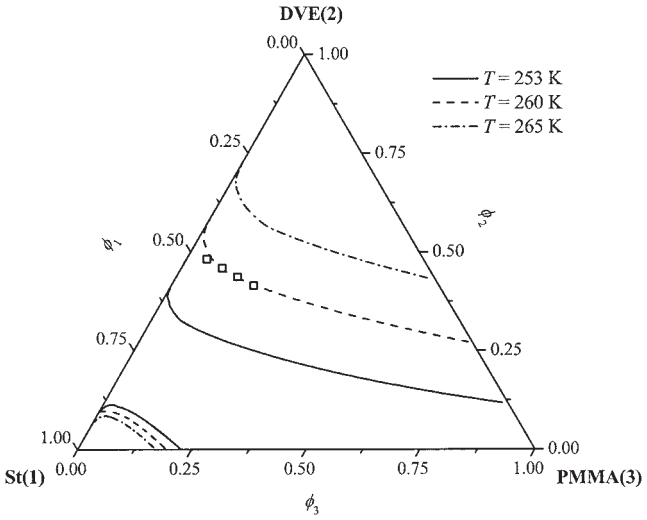

Figure 8 Calculated quasiternary CPCs at different temperatures, and (□) global compositions of prepared materials with 5, 10, 15, and 20 wt % PMMA on a constant weight proportion of St:DVE = 45:55 wt %.

should be represented by means of a quaternary phase diagram that describes the phase evolution by effect of the increasing conversion that change the concentration of the four components. The St and DVE comonomers concentration diminishes, and that of the St-*co*-DVE copolymer increases, whereas that of the modifier remains unchanged.

At a fixed conversion below the gel point, the St-*co*-DVE copolymer formation contributes to increase the incompatibility with the St and DVE monomers, as well as with the PMMA modifier. This effect is originated by the different energy interaction values for the contacts of each St and DVE comonomer segments in the copolymer molecule with respect to contacts between the segments of the other three components, St, DVE, and PMMA molecules. This effect is superposed to a reduction in the entropic contribution to the Gibbs free energy. The net result is to increase the immiscibility surface area in the quaternary tetrahedron phase diagram, which enclose the immiscibility volume region. Up to the conversion gel point, the elastic free energy contribution increases even more the immiscibility volume region inside the surface phase diagram.

Because of the high initial miscibility of the system St-DVE-PMMA, the conversion in the pregel region of the crosslinking reaction has to progress significantly, for the immiscibility surface area to grow enough to superpose to the points representing the global compositions of the system (points in Fig. 8). When these points are reached, the entire material suffers the phase separation process by a polymerization-induced phase separation (PIPS) mechanism. In consequence, the final morphologies of the obtained materials are the result of the phase separation originated by the PIPS mechanism from an initially homogeneous reaction mixture.

Figure 9(a,b) shows the SEM micrographs of the fracture surfaces for the cured materials modified with 5 and 20 wt % PMMA, respectively. Figure 10(a,b) shows the TEM micrographs of the same samples.

To recognize the major component present in each phase of the TEM micrographs, a PMMA-modified St-DVE thermoset with macrophase separation was observed by TEM in the same conditions. This material was obtained using both a commercial DVE (M_n = 1015 g/mol, M_w/M_n = 1.74) and a PMMA modifier of high molar mass and polydispersity index (M_n = 239,000 g/mol, M_w/M_n = 2.68). The origin of this morphology has been discussed in a previous work.[21] Figure 11 corresponds to the TEM micrograph of this sample, which shows the St-*co*-DVE copolymer-rich phase as dark gray areas while the PMMA-rich phase looks light gray. This gray contrast can be explained in function of the different local electronic densities between both phases.[25,26] The π-conjugate electronic structure of the aromatic rings contained in the St and DVE comonomers forming the copolymer will scatter more electrons from the primary electronic beam than the PMMA aliphatic chains, for the same specimen thickness. As a result, St-*co*-DVE copolymer-rich regions will appear darker in the image. SEM micrograph reported for the same system,[21] shows two well-differentiated regions: a St-*co*-DVE copolymer-rich continuous phase (dark gray area in TEM) and a discontinuous PMMA-rich phase in the form of drop-like regions of 30–100 ìm size (light gray area in TEM) with a very complex "salami type" internal microstructure constituted by St-*co*-DVE copolymer nodules of 1–5 ìm size (dark gray microinclusions).

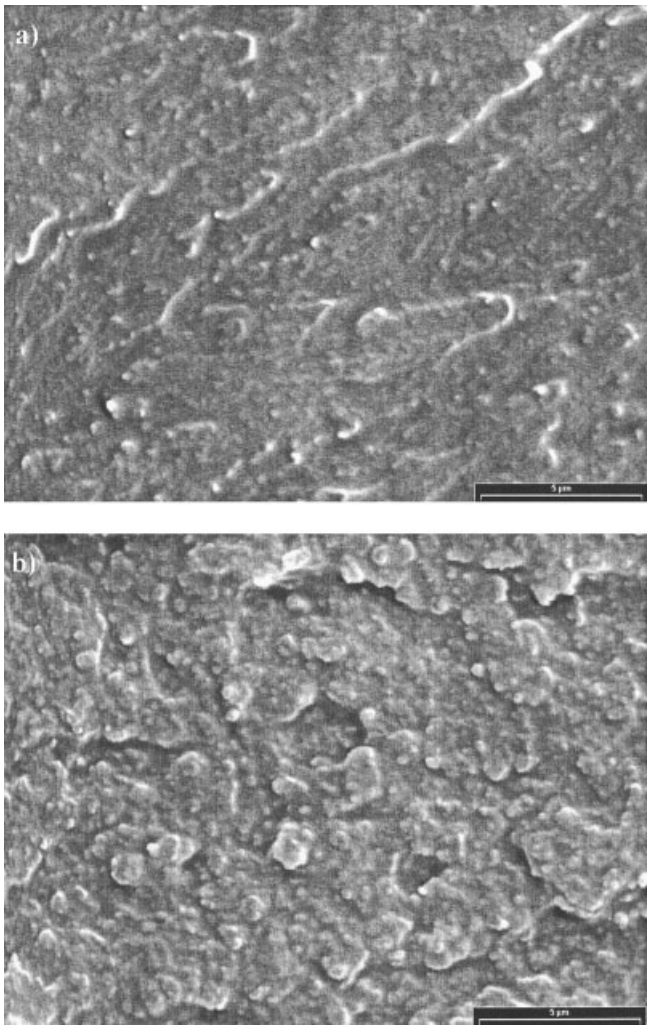

Figure 9 SEM micrographs (at ×6000) of the fracture surfaces for the cured St-DVE materials modified with: (a) 5 wt % PMMA and (b) 20 wt % PMMA.

This study allows to interpret the TEM and SEM micrographs of the materials obtained in the present work. Figure 9(a) (5 wt % PMMA) shows a rough fracture surface with very small nodules fused on the sample surface. SEM image is consistent with the TEM indication [Fig. 10(a)] of a fine dispersion of PMMA microparticles distributed in a St-*co*-DVE continuous

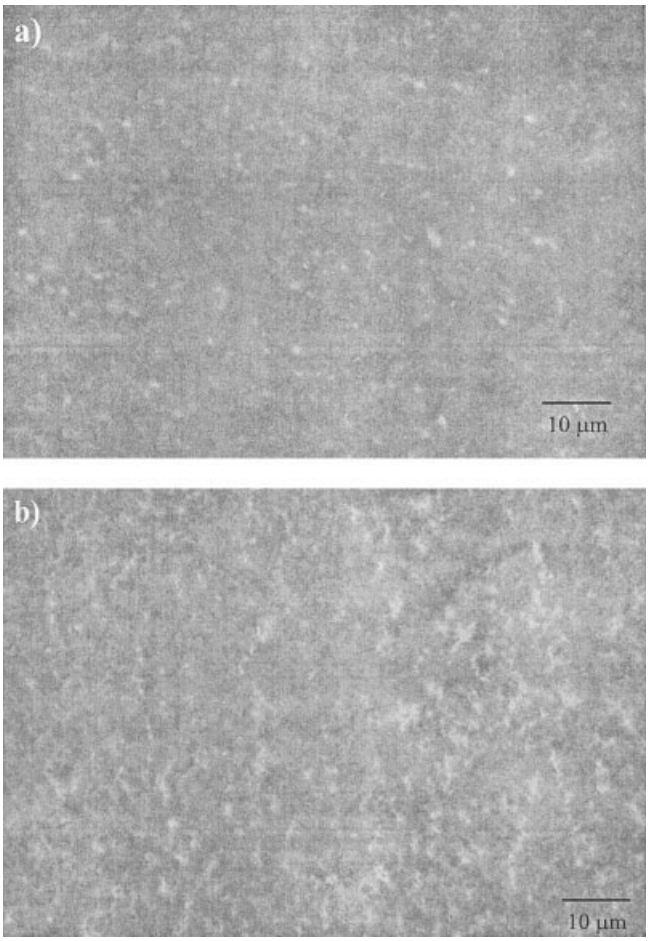

Figure 10 TEM micrographs (at ×10,000) of the cured St-DVE materials modified with: (a) 5 wt % PMMA and (b) 20 wt % PMMA.

phase, which permits to explain the macroscopically observed translucence of this sample.

On the other hand, SEM of sample with 20 wt % PMMA [Fig. 9(b)] shows a very irregular surface consisting of aggregates of irregular nodular particles with diameters in the range of 0.1–1 μm. These nodules are formed by St-*co*-DVE crosslinked copolymer, and surrounding the nodular aggregates is the PMMA-rich phase, as shown by the light gray areas in Figure 10(b). This sample (20 wt % PMMA) is opaque after cure.

Figure 12 is a schematic drawing of the evolution of the last morphologies (Fig. 10), as the degree of reaction advances. Initially, the system is formed by a homogeneous mixture of the comonomers and the modifier [Fig. 12(a)]. At low conversions, nanogels are formed by the reaction of the resin and St [Fig. 12(b)]. These nanogels aggregate and coreact through surface unsaturations, forming much larger microgels, which further interact and react with each other, forming nodules on the order of microns that can be easily seen by electron microscopy [Fig. 12(c)]. As the reaction proceeds, the nodules touch each other and form the main phase, rich on the St-DVER copolymer. The modifier that has been rejected towards the exterior of these nodules during the reaction (due to the increasing incompatibility with the formed copolymer) is finally confined to the interstices left in between the "reaction aggregated" nodules [Fig. 12(d)].

Previous studies on St-DVE thermosets modified with elastomers[5,14,27] or St-UP systems modified with different thermoplastics,[7,12,28] in the range of 5–15 wt % modifier, have shown similar morphological features as those presented in this work.

As it was already explained, the phase separation by PIPS mechanism needs a significant progress in conversion of the crosslinking reaction in the pregel region because of the high initial miscibility of the St-DVE-PMMA system. As a consequence, the phase-separation process is quickly arrested by the increase in the viscosity in the pregel state or by gelation in the postgel state, giving place to small nodular particle aggregates of St-*co*-DVE copolymer with poorly defined interfaces, as shown clearly in Figures 9 and 10.

CONCLUSIONS

Under the F-H theory framework, measured cloud point for the St(1)-PMMA(3) quasibinary and the St(1)-DVE(2)-PMMA(3) quasiternary at three different temperatures were used to calculate the χ_{13} and χ_{23} binary interaction parameter. DVE and PMMA polydispersities were taken into account during quasibinary and quasiternary calculations. Definition of pseudocomponents from the DVE and PMMA SEC mass-fraction distributions was an effective method to keep discrete distributions, while reducing computing time for the interaction parameters calculation. The

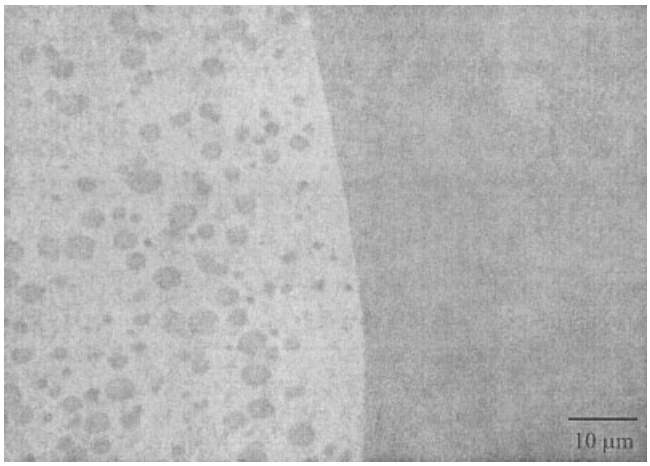

Figure 11 TEM micrograph (at ×10,000) of a cured St-DVE material modified with 10 wt % PMMA, using both DVE and PMMA of higher molar mass and polydispersity index.[21]

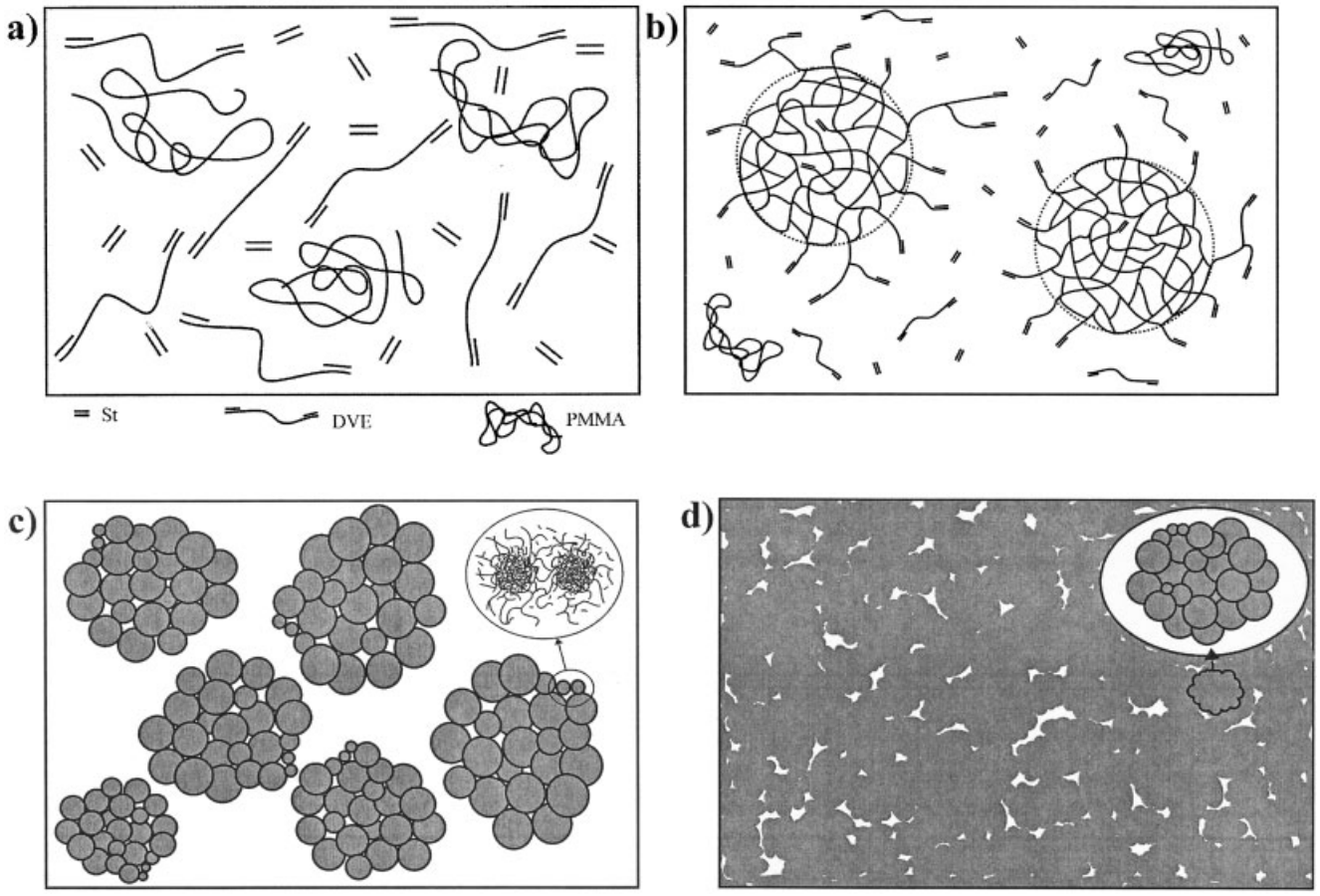

Figure 12 Schematic drawing of the evolution of the morphologies shown in Figure 10, as the degree of reaction advances.

miscibility of St-PMMA is little affected by the increase in molar mass and polydispersity of PMMA. The increase in DVE molar mass produces a displacement of DVE-PMMA binary cloud-point phase diagram to higher temperatures, thereby increasing the system immiscibility. The calculated χ-parameters were of great value to predict the quasiternary phase diagrams at different temperatures. At low temperatures, the quasiternary system shows liquid–liquid partial miscibility on the St-PMMA and DVE-PMMA binary sides, while at temperatures above room temperature, the system is completely miscible at all compositions.

Predicted quasiternary phase diagrams give useful information to correlate initial miscibility of PMMA-modified St-DVE reaction system with the final morphologies of the crosslinked materials. The developed morphologies are the result of the phase separation originated by the PIPS mechanism from an initial homogeneous mixture. Phase separation occurs after a significant progress in the crosslinking reaction conversion, because of the high initial miscibility of the St-DVE-PMMA system. As a consequence, the phase separation process is quickly arrested by gelation, which gives place to the formation of small nodular particle aggregates of St-*co*-DVE copolymer with poorly defined interfaces.

References

1. Zawke, S. H. In Handbook of Thermosetting Resins; Goodman, S. H., Ed.; Noyes Publications: New Jersey, 1986; Chapter 1.
2. Pascault, J. P.; Williams, R. J. J. In Polymer Blends; Paul, D. R., Bucknall, C. B., Eds.; Wiley: New York, 2000; Vol. 1, Chapter 13.
3. Suspense, L.; Yang, Y. S.; Pascault, J. P. In Toughened Plastics I: Science and Engineering; Riew, C. K.; Kinloch, A. J., Eds.; American Chemical Society: Washington, DC, 1993; Advances in Chemistry Series 233, Chapter 7.
4. Auad, M. L.; Aranguren, M. I.; Borrajo, J. J Appl Polym Sci 1997, 66, 1059.
5. Auad, M. L.; Frontini, P. M.; Borrajo, J.; Aranguren, M. I. Polymer 2001, 42, 3723.
6. Ullett, J. S.; Chartoff, R. P. Polym Eng Sci 1995, 35, 1086.
7. Dong, J. P.; Huang, J. G.; Lee, F. H.; Roan, J. W.; Huang, Y. J. J Appl Polym Sci 2004, 91, 3369.
8. Wang, S.; Wang, J.; Ji, Q.; Schultz, A. R.; Ward, T. C.; McGratz, J. E. J Polym Sci Part B: Polym Phys 2000, 38, 2409.
9. Gryshchuk, O.; Jost, N.; Karger-Kocsis, J. J Appl Polym Sci 2002, 84, 672.
10. Karger-Kocsis, J.; Fröhlich, J.; Gryshchuk, O.; Kautz, H.; Frey, H.; Mülhaupt, R. Polymer 2004, 45, 1185.
11. Suspene, L.; Fourquier, D.; Yang, Y. S. Polymer 1991, 32, 1593.
12. Huang, Y. J.; Su, C. C. J Appl Polym Sci 1995, 55, 305.

13. Huang, Y. J.; Jiang, W. C. Polymer 1998, 39, 6631.
14. Auad, M. L.; Aranguren, M. I.; Borrajo, J. Polymer 2001, 42, 6503.
15. Robinette, E. J.; Ziaee, S.; Palmese, G. R. Polymer 2004, 45, 6143.
16. Li, L.; Sun, X.; Lee, L. J. Polym Eng Sci 1999, 39, 646.
17. Li, W.; Lee, J. L. Polymer 2000, 41, 697.
18. Huang, Y. J.; Liang, C. M. Polymer 1996, 37, 401.
19. Kamide, K. In Thermodynamics of Polymer Solutions: Phase Equilibria and Critical Phenomena; Jenkis, A. D., Ed.; Polymer Science Library 9; Elsevier: Amsterdam, 1990; Chapters 4,5.
20. Kamide, K.; Matsuda, S.; Shirataki, H. Eur Polym J 1990, 26, 379.
21. Schroeder, W. F.; Auad, M. L.; Barcia Vico, M. A.; Borrajo, J.; Aranguren, M. I. Polymer 2005, 46, 2306.
22. Ziaee, S.; Palmese, G. R. J Polym Sci Part B: Polym Phys 1999, 37, 725.
23. Shirataki, H.; Kamide, K. Polym Int 1993, 32, 265.
24. Rätzsch, M. T. Makromol Chem Macromol Symp 1987, 12, 101.
25. Sawyer, L. C.; Grubb, D. T. In Polymer Microscopy; Chapman & Hall: London, 1996; Chapter 3.
26. Williams, D. B.; Barry Carter, C. In Transmission Electron Microscopy; Plenum: New York, 1996; Vol. 3, Chapter 22.
27. Auad, M. L.; Proia, M.; Borrajo, J.; Aranguren, M. I. J Mater Sci 2002, 37, 4117.
28. Hsu, C. P.; Kinkelaar, M.; Hu, P.; Lee, L. J. Polym Eng Sci 1991, 31, 1450.